Defence Science Journal, Vol. 73, No. 1, January 2022, pp. 112-116, DOI : 10.14429/dsj.73.1.18120

Analysis of Pleated Discrete Pore Non-Woven Layer Type Filter Element for Naval Applications

P.S. Chenthil Prabu*, Chellapilla Vamsi Krishna, S. Nagesh, R.P. Chandrasekhar and R. Murugesan

DRDO-Combat Vehicle Research and Development Establishment, Avadi, Chennai - 600 054, India,

**E-mail: cprabu.ps@gmail.com*

ABSTRACT

In naval applications generally, the pleated discrete pore non-woven layer filter element is used. Filters used for such applications require a maximized filtration rate, lower pressure drop, higher permeability, effective pore size distribution and good filtration efficiency. In the other most common wire mesh filter element type, the geometric parameters are well-defined and can easily be modelled. In the case of non-woven layer filter element, the pores are arranged in a randomly distributed manner and the modelling becomes difficult. In this present study, a new approach was contemplated for modelling the same. The fluid flow through the filter element is by percolation phenomenon. Using Darcy's law approach, the pressure drop across the filter element for different flow rates was found analytically by considering the flow resistance in all three polar coordinates r, θ and Z. The theoretical prediction made by CFD analysis is correlated with actual model behaviour and a good degree of correlation is obtained which shows the efficacy of this method for wider use in similar applications.

Keywords: Darcy's law; Percolation; Pleated discrete pore non-woven layer; CFD analysis

1. INTRODUCTION

In a filter, the filter medium controls the filtration process and the properties of the filter medium determine how the filter performs to remove the particles from the fluid. A special sub-category of non-woven fibre element is made out of glass fibre media[1,6,10]. The limitation of glass media is that it has high specific resistance and limited mechanical strength. To offset the former, the filter element is most commonly used in pleated form to increase the superficial area for a given size of the element. This increase in area facilitates more flow through the element resulting in the reduction of overall flow resistance offering a pressure drop. The pleating of an element will also improve its rigidity of the element, although it is normally supported by a perforated inner tube or core. The pleated type of glass media mesh can tolerate extreme thermal ranges and differential pressures along with excellent dirt-holding capacity[2,5,10]. In the wire mesh type of element, the geometric parameters are well-defined and can easily be modelled, whereas for a non-woven layer filter, the pores are arranged in a randomly distributed way and the creation of a geometric model is difficult[3]. The filter is considered as porous media with porosity or void fraction arriving from the resistance offered to fluid flow. Considering this, the present method has evolved.

2. METHODOLOGY

The pleated filter element is characterised based on geometric parameters such as pleat width (thickness), pleat length, pleat bending radius and angle. In filter media, some important properties such as porosity and permeability are required to be defined and usually determined under experimental conditions[1,7]. In this analytical method, the filter media is modelled as the porous media using Darcy's Law in the CFD code. The fluid flow through the filter element can occur from the outward to the inward direction or vice versa[4]. The pressure drop across the pleated filter element is due to permeability and porosity. To model the pleated filter, the entire filter element is assumed as a hollow cylinder so that the flow occurs radially across the pleated filter element which is equivalent to the pleat length of known pleat width. In this, the flow is expected to occur only in the radial direction of the filter element. Flow is provided in one direction and restricted in the other directions. Varying the flow rate as a boundary condition in the CFD simulation, the pressure drop has been estimated. CFD solves the partial differential equations into algebraic equations by satisfying the conservation laws of mass, momentum and energy equations.

3. MODELING OF DISCRETE PORE

The fluid flowing into the filter element has to face two different resistances i.e. inertial resistance and viscous resistance. These two resistances define the porosity of the medium. The inertial and viscous resistances are obtained using a characteristic curve from the pressure drop versus velocity.

The calculation of inertia and viscous resistance is given by:

Pressure drop across the porous media as per Darcy's law:

Received : 25 April 2022, Revised : 18 October 2022
Accepted : 05 January 2023, Online published : 10 March 2023

$$\Delta P = \frac{1}{2}\rho C_2 t V^2 + \left(\frac{\mu}{\alpha}\right) tV \tag{1}$$

Where,

μ - Dynamic viscosity, kg/m-s

A - Permeability, m^2

V - Velocity, m/s

ρ - Density, kg/m^3

C_2 - Inertial resistance factor, 1/m

t - Thickness of porous media, m

The polynomial fit equation is obtained from the pressure drop versus velocity curve which can be represented as

$$\Delta P = AV^2 + BV + C \tag{2}$$

Where,

C=0

Comparing Eqns. (1) & (2),

$$A = \frac{1}{2}\rho C_2 t \text{ (Kg/m}^3\text{)} \tag{3}$$

i.e., Inertial Resistance

$$C_2 = \frac{2A}{\rho t} (1/m) \tag{4}$$

$$B = \left(\frac{\mu}{\alpha}\right) t \text{ (Kg/m}^2\text{s)} \tag{5}$$

i.e., Viscous Resistance

$$\alpha^{-1} = \frac{B}{\mu t} (1/m^2) \tag{6}$$

Using Eqn. (5) and Eqn. (6) the inertial and viscous resistance is calculated. The single pleat element has been considered for analysis[1-4] as shown in Fig. 1 to Fig. 3.

H= Height of the pleat

D=Diameter of the pleat

Figure 1. Arrangement of filter element pleat.

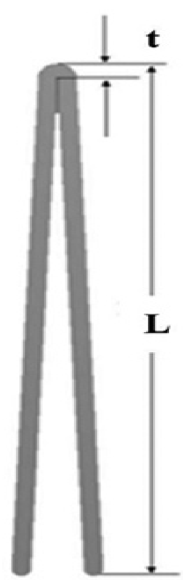

L=Length of the pleat
t= Thickness of the pleat

Figure 2. Single pleat.

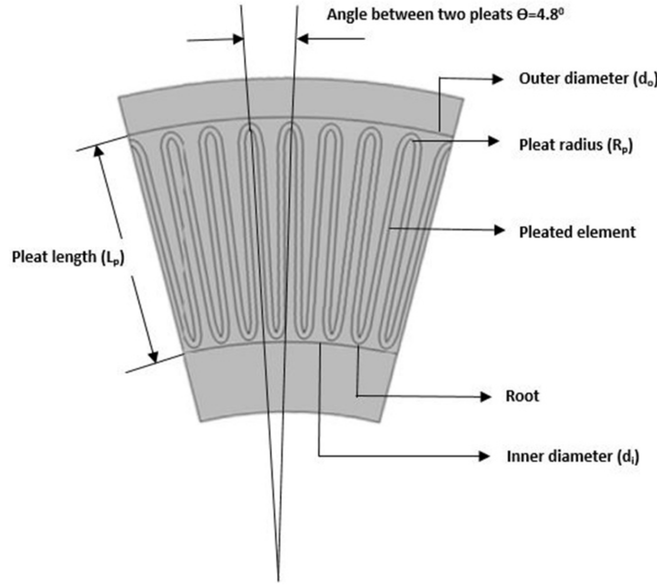

Figure 3. Layout of specific pleat element used for analysis.

3.1 Influence of Pleat radius/Curvature Effect

The required number of pleats is arranged using a pleat radius to have desired increase or decrease of the pressure drop. The curvature of the pleat radius influences the pressure drop in the filter element which will optimize the filtration rate. An increase in the number of pleats increases in viscous resistance offered by the fluid thereby the increase in pressure drop.

3.2 Layering

The pleats are arranged in layers to maximize the filtration rate and allow the impurities to segregate in the membrane of the filter.

4. CASE STUDY

For the case study, a hydraulic filter of out-to-in type is considered with the pleated element. To obtain the polynomial equation the pressure drop versus velocity details across the filter element needs to be known. The following procedure is adopted to get the characteristic curve of the pleated mesh (filter element) considering a specific pleat characteristic. In this specific pleat Velocity versus Pressure drop, characteristics were synthesized using commercial CFD code ANSYS version 2019 R3. In this analysis the turbulent k– ε model is used to estimate the pressure drop value[11]. Figure 4. Shows the layout of the filter element.

The k-ε model takes into account the turbulence effect away from the wall which can give better results instead of using the k-ω model which considers the turbulences near the wall. In the k-ε model with the standard method, realizable and non-equilibrium wall function is used in the analysis which reduces the number of cells to be iterated. The Hybrid initialization method is used as the initialization technique for the solution because of two parameters to be specified.

The characteristic curve fitting is carried out using a second-degree polynomial equation. This CFD procedure only predicts flow characteristics for a single pleat, further taking into account the total number of pleats the filter media

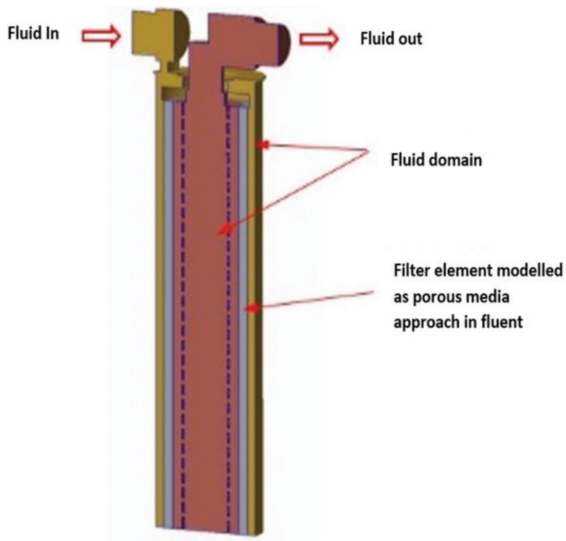

Figure 4. Layout of filter.

permeability and filtration rating is estimated. The estimated filtration may be in agreement with the actual.

The equation is

$$y = 0.0177x^2 + 0.0015x \qquad (7)$$

From the equation, A=0.0177 and B=0.0015. Since the pressure drop is plotted in the bar, A and B have to solve for the SI unit. Which gives *A*=1770 and *B=150*.

Using Eqn. (4) and Eqn. (6), calculate C_2 as 9593.495 (1/m) & α^{-1} as 28627046.833 (1/m^2) respectively.

Viscous resistance for the total number of pleats, α^{-1} is 2147028512.475(1/m^2).

Permeability $\alpha = 4.65 * 10^{-10}$ (m^2)

Filtration rating = 24.66 μm

Where,

ρ - Density of liquid = 900 kg/m^3

t - Thickness of the porous media = 0.00041m

μ - Dynamic viscosity = 0.01278 kg/m-s

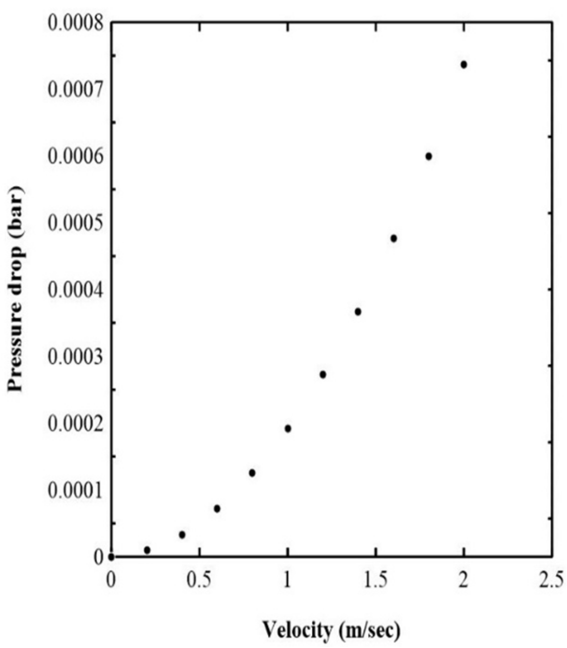

Figure 5. Estimated characteristic flow curve for porous media.

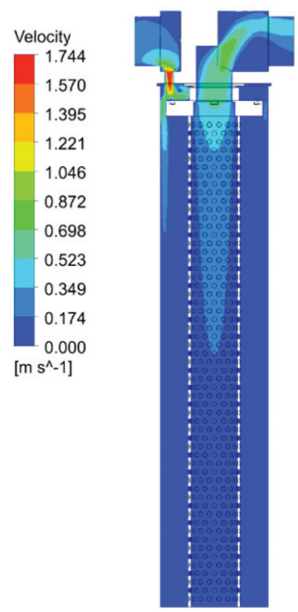

Figure 6. Velocity contour.

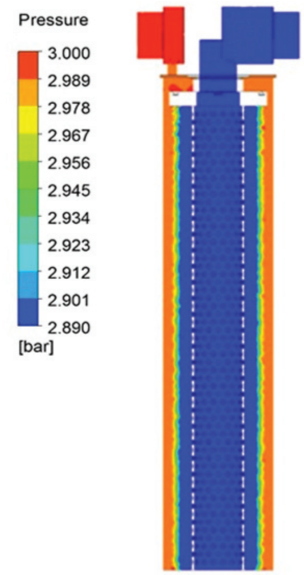

Figure 7. Pressure contour.

Table 1. The typical pressure drop obtained for different velocities across the element

Sr. No	Velocity (m/sec)	Pressure drop (bar)
1	0	0
2	0.2	0.0000095
3	0.4	0.0000337
4	0.6	0.0000722
5	0.8	0.0001248
6	1.0	0.0001915
7	1.2	0.0002722
8	1.4	0.0003671
9	1.6	0.0004760
10	1.8	0.0005990
11	2.0	0.0007361

From this, inertial resistance and viscous resistance have been found. The Estimated characteristic flow curve for porous media is shown in Fig. 5.

Using the porous media approach for the entire filter element the flow versus pressure drop curve is obtained using the CFD. Pressure drop is estimated for different flow rates starting from 0 to 100 lpm shown in Table 2. The velocity contour and pressure contour to one such flow rate are shown in Fig. 6 and Fig. 7.

It is observed that the maximum velocity occurs at the narrow portion of the inlet side in Fig. 6. The maximum pressure occurs on the inlet side and the minimum pressure at the outlet due to permeability as shown in Fig. 7.

5. EXPERIMENTAL VALIDATION

To validate the method, an experiment has been conducted to correlate the results. In this test setup, the test unit was connected to a hydraulic test bench. The inlet side is connected to the pump. The outlet is connected to the tank. The flow at the inlet is maintained in steps and after flow stabilization, the inlet and outlet pressure are measured. The algebraic difference between the pressures gives the pressure drop for the variable flow rates. The test filter is shown in Fig. 8. The experimental validation was carried out to estimate the pressure drop using the flow versus pressure drop test as shown in Fig. 9. The correlation between theoretical and model behavior is shown in Fig. 10. A good degree of correlation is obtained.

Figure 8. Test filter.

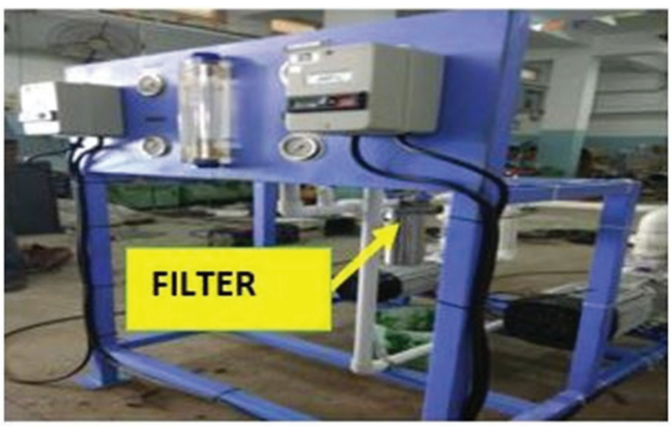

Figure 9. Experimental test setup used to measure the flow vs pressure drop.

Table 2. The pressure drop obtained for different fluid flow rates for filter assembly

Flow rate (l pm)	Pressure drop (bar)	
	Analysis	Experiment
0	0	0
20	0.1437	0.11
50	0.3957	0.35
75	0.6176	0.56
100	0.8454	0.80

6. DISCUSSION

The pressure drop across the filter with different flow rates was obtained and the correlation between theoretical prediction versus model behaviour shows that both the pressure drop results were in agreement with each other for the non-woven layer filter element. The pressure drop value is of higher bound value in the analysis because of the very high resistance offered by the fluid in two directions other than the radial direction. Whereas in practice, flow occurs in all directions.

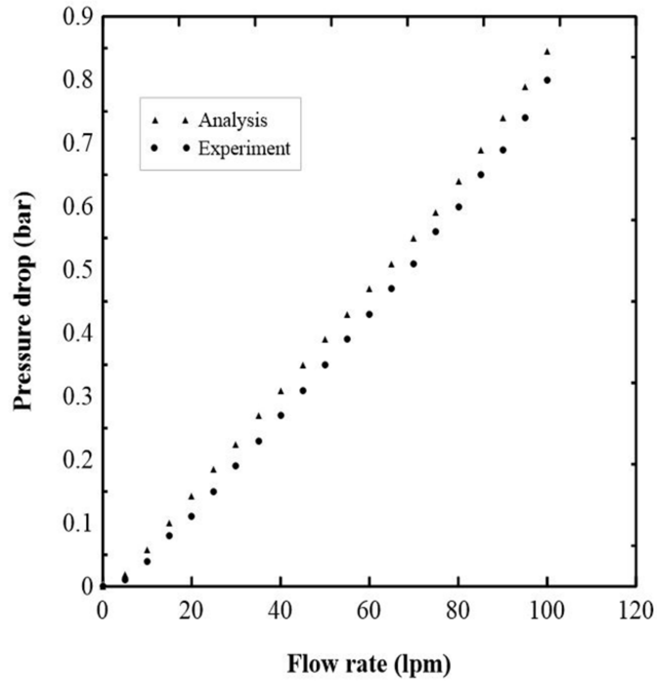

Figure 10. Correlation between theoretical prediction and model behaviour.

7. CONCLUSION

From the study, it is found that the simulation results of the k–ε turbulence model used in this analysis are in agreement with experimental values. The pressure drop across the filter element is increased with decreasing porosity. The increase in the length of the pleat causes an increase in the filtration area and decreases the pressure drop. The theoretical prediction by CFD simulation was correlated with model behaviour. A good degree of correlation obtained shows the efficacy of this method for wide use in a similar application. This method can be readily used in new filter designs, with great potential of reducing the need for prototype and testing resulting in cost and time reduction.

REFERENCES

1. Velali, Eirini; Dippel, Jannik; Stutem, Birgit; Handt, Sebastian; Loewe, Thomas & Lieres, Eric Von. Model-based performance analysis of pleated filters with non-woven layers. *Separation and Purification Technol.*, 2020, **250**, 1-10. doi:10.1016/j.seppur.2020.117006
2. Wiegmann, Andreas; Rief, Stefan & Kehrwald, Dirk. Computational study of pressure drop dependence on pleat shape and filter media. *Filtration & Separation Technol*, 2007, 79-86.
3. Pejmansanaei, Yixuan sun; Kondic, Lou & Cummings, L.J. Modeling and design optimization for pleated

membrane filters. *Phys. Rev. Fluids*, 2019.
doi: 10.48550/arXiv.1911.11320
4. Sanaei, P.; Richardson, G.W.; Witelski, T. & Cummings, L.J. Flow and fouling in a pleated membrane filter. *J. Fluid Mechanics,* 2016, 36-59.
doi: 10.1017/jfm.2016.194
5. Wiegmann, Andreas; Rief, Stefan; Latz, Arnulf & Oleg, Iliev. Toward predicting filtration and separation. *Progress & Challenges*, 2009, 1-16.
6. Dippel, Jannik; Handt, Sebastian; Stute, Birgit & Loewe, Thomas. Fluid dynamics in pleated membrane filter devices. *Separation and Purification Technol.*, 2021, **267**(1-2).
doi:10.1016/j.seppur.2021.118580
7. Theron, Felicie; Joubert, Aurelie, Laurence, Le Coq. Numerical and experimental investigations of the influence of the pleat geometry on the pressure drop and velocity field of a pleated fibrous filter. *Separation and Purification Technol.*, 2017, 69-77.
doi: 10.1016/j.seppur.2017.02.034
8. Wakeman, Richard & Tarleton, Stephen. Solid/ Liquid Separation: Principles of Industrial Filtration. Elsevier, USA, 2005. 340 p
9. Sparks, Trevor & Chase, George. Filters and filtration Handbook. Sixth Edition. Elsevier, USA, 2015. 444 p.
doi: 10.1016/C2012-0-03230-9
10. Irwin M., Hutten. Handbook of Nonwoven Filter Media. Second edition, Elsevier, USA, 2015. 674 p.
doi: 10.1016/C2011-0-05753-8
11. ANSYS® Fluent, Release 19.3, Help system, ANSYS Fluent Theory Guide, ANSYS, Inc.

ACKNOWLEDGEMENT

The authors are grateful to Sri Balamurugan V, Director, CVRDE for his guidance, support and encouragement. The authors are also grateful for the contributions made by divisions of AP and CEAD of CVRDE.

CONTRIBUTORS

Mr P.S. Chenthil Prabu obtained his Post-Graduation from Bharathidasan University. He is working as a Scientist at DRDO-CVRDE. His area of interest includes thermo-mechanical analysis, heat transfer analysis, structural analysis, size optimization and internal flow simulation.
For this study, he formulated this technique for the filter element to perform the CFD simulation and demonstrated it.

Mr Chellapilla Vamsi Krishna obtained his Post-Graduation from JNTU. He is working as a Senior Research Fellow at DRDO-CVRDE. His area of research includes CFD analysis and conjugate heat transfer analysis.
For this study, he has applied this current method and carried out the numerical CFD simulation.

Dr S. Nagesh obtained his PhD from the Defence Institute of Advanced Technology (Deemed University), Pune. He is working as a Scientist at DRDO-CVRDE. Presently, he is handling a project for the development of high-speed flexible coupling for aircraft applications and the development of critical filters for aeronautical & marine applications.
For this study, he is the Project Manager for Filter Development who approved this approach.

Mr R.P. Chandrasekhar obtained his Post-Graduation from Anna University. He is working as a Scientist at DRDO-CVRDE. Presently, he is handling the project for the development of filters for marine and aircraft applications.
For this study, he has conducted experimental validation to verify the CFD simulation results.

Mr R. Murugesan obtained his Post-Graduation from Anna University. He is working as a Scientist at DRDO-CVRDE. He is the Additional Director, in-charge of the Centre for Engineering Analysis and Design.
For this work, he has reviewed and guided this task to establish the methodology.